water

MDPI

Review

The Effect and Adjustment of Ferrate Species in Ferrate-Based Advanced Oxidation Processes for Wastewater Treatment: A Systematic Review

Yushu Wang [1,†], Xiao Luo [1,†], Xiaoke Ma [1], Patiya Kemacheevakul [2], Sen Qu [1], Junxiang Huang [1], Tarloh G. Chea [1], Peizhe Sun [1,3], Lin Zhao [1,3], Youjun Zhang [1] and Yongkui Yang [1,3,*]

[1] School of Environmental Science and Engineering, Tianjin University, Tianjin 300350, China; yushuwang@tju.edu.cn (Y.W.); 2021214032@tju.edu.cn (X.L.); maxiaoketju@163.com (X.M.); qusen2000@163.com (S.Q.); huangjunxiang0828@163.com (J.H.); cheatarloh@gmail.com (T.G.C.); sunpeizhe@tju.edu.cn (P.S.); zhaolin@tju.edu.cn (L.Z.); zhangyoujun001@126.com (Y.Z.)
[2] Department of Environmental Engineering, Faculty of Engineering, King Mongkut's University of Technology Thonburi, Bangkok 10140, Thailand; patiya.run@gmail.com
[3] China-Singapore Joint Center for Sustainable Water Management, Tianjin University, Tianjin 300350, China
* Correspondence: ykyang@tju.edu.cn; Tel.: +86-22-87402072
† Yushu Wang and Xiao Luo contributed equally as the first authors of this manuscript.

Abstract: Interest in the combination of ferrates and advanced oxidation processes (AOPs) for wastewater treatment has increased, as revealed in this systematic review. In this study, the multiple functions of Fe(VI) in ferrate-based AOPs are summarized based on the Fe species. Various enhanced oxidation pathways are achieved through electron capture by Fe(VI), oxidation by Fe(V) and Fe(IV), or the catalytic effects of Fe(III) and Fe(II). The different contributions of high-valent Fe species and general reactive oxidation species are highlighted by analyzing the results of quenching, methyl phenyl sulfoxide probing, and electron paramagnetic resonance analysis. Methods that are used to adjust the Fe species, including changing the reaction pH, oxidant dosage, dosing pattern, and the addition of reducing or complexing additives, can influence the enhancement efficiency of micropollutant treatment from the perspective of determining the transformation from Fe(VI) to Fe(V) and Fe(IV) with higher reactivity or Fe(III) and Fe(II) circulation. Future studies should focus on the in situ production of high-valent Fe and oxidation pathway-based adjustments in Fe(VI)-AOP techniques.

Keywords: ferrate; advanced oxidation processes (AOPs); Fe species adjustment; wastewater treatment

check for updates

Academic Editors: Yung-Tse Hung, Issam A. Al-Khatib, Rehab O. Abdel Rahman, Tsuyoshi Imai and Qaisar Mahmood

Received: 8 April 2025
Revised: 27 April 2025
Accepted: 27 April 2025
Published: 30 April 2025

Citation: Wang, Y.; Luo, X.; Ma, X.; Kemacheevakul, P.; Qu, S.; Huang, J.; Chea, T.G.; Sun, P.; Zhao, L.; Zhang, Y.; et al. The Effect and Adjustment of Ferrate Species in Ferrate-Based Advanced Oxidation Processes for Wastewater Treatment: A Systematic Review. *Water* **2025**, *17*, 1343. https://doi.org/10.3390/w17091343

Copyright: © 2025 by the authors. Licensee MDPI, Basel, Switzerland. This article is an open access article distributed under the terms and conditions of the Creative Commons Attribution (CC BY) license (https://creativecommons.org/licenses/by/4.0/).

1. Introduction

The removal of emerging contaminants such as pharmaceuticals, personal care products, and endocrine-disrupting chemicals from wastewater has generated great interest in the past few years. Advanced oxidation processes (AOPs) have been reported to effectively remove micropollutants by producing free radicals such as sulfate radicals and hydroxyl radicals with high redox potentials. Non-radical oxygen species such as singlet oxygen ($^1O_2$) also contribute under certain conditions [1]. AOP techniques using O_3, H_2O_2, peroxymonosulfate (PMS and HSO_5^-), and peroxydisulfate (PDS, $S_2O_8^{2-}$) as precursors and light, carbon-derived materials, and metal ions as activators have been reported [2–4]. However, traditional AOPs depend significantly on the catalytic process [5] and are limited to a narrow pH range [6]. Moreover, concerns have arisen about their non-selective oxidation,

which is attributed to the generation of disinfection byproducts [7] and slow reactions with micropollutants in water with a strong background of natural organic matter [8].

High-valent Fe species (Fe(VI), Fe(V), and Fe(IV)) have drawn wide attention because they have a high oxidation capacity and low risk [9]. Fe(VI) shows great potential for pollutant removal via oxidation [10], coagulation, and disinfection [11], with the resulting Fe(III)/Fe(II) species exhibiting catalytic effects [3]. However, its practical application is limited by its rapid decomposition at a neutral pH and its low reactivity under basic conditions [12]. Different ferrate techniques have been assessed for the treatment of emerging organic pollutants [13] and to clarify the mechanisms and kinetics of pollutant removal [14,15]. The contribution of Fe(VI) to total organic carbon (TOC) removal and the inhibition of disinfection byproducts during water and wastewater treatment has been highlighted [16]. Recent review articles have elucidated Fe(VI) activation methods, focusing on the production of Fe(V) and Fe(IV) by metal ions [17] and inorganic reductants [18]. Iron-based materials are commonly used to activate AOPs owing to their high catalytic performance and environmental compatibility. Consequently, Fe(VI) decomposition products, including Fe(III) and Fe(II) ions, as well as FeOOH, Fe_2O_3, and Fe_3O_4, have been reported to be effective activators of AOPs precursor oxidants [19] and as feedstock for Fe(IV) generation [20]. These Fe species serve as potential connections between Fe(VI) and AOPs, through which the disadvantages of the two individual oxidation techniques can be mitigated [21]. In 2010, Sharma innovatively summarized the Fe(VI)-enhanced photocatalytic oxidation reaction [22], and subsequently highlighted the oxidation contributions of Fe(V) and Fe(IV) to these systems [18]. Further investigations into the oxidation mechanisms of ferrate-AOPs have emerged, focusing on various aspects such as oxidation kinetics, contaminant removal efficacy [23,24], and optimized ferrate-AOP techniques [25,26]. Recently, attention has been drawn to the formation of multiple reactive species in ferrate-AOPs, including high-valence Fe species and radicals [27,28]. However, comprehensive reviews on the reaction mechanisms of different Fe species, their transformation processes, and their adjustment measures are currently lacking.

This review aims to (1) demonstrate the different roles of Fe species under different ferrate-AOP conditions and describe the corresponding mechanisms by which the processes are enhanced and (2) discuss methods to optimize the ferrate-AOP by adjusting the Fe species in the system.

2. Key Fe Species in Ferrate-Based AOP Systems

The self-decay of Fe(VI) is accompanied by the removal of organic pollutants and the production of catalysts, such as Fe(III) and Fe(II), which provide a bridge connecting AOPs to Fe(VI) oxidation. A comprehensive understanding of the behavior of Fe intermediates in ferrate-AOPs will guide the development of improved pollutant removal systems and facilitate the application of this combined system to complex practical wastewater treatment.

Various transient reactive species, including Fe(V), Fe(IV), and free radicals, are generated in the oxidation reaction system. Fe(VI) self-decomposes in pure water to Fe(V) and Fe(IV). The synergistic effects of reducing agents with Fe(VI) could enhance the formation of Fe(IV) and Fe(V). Sulfur-containing compounds could activate Fe(VI) to generate reactive Fe(V) and Fe(IV) intermediates, thereby augmenting the oxidative capacity of the Fe(VI) system via the in situ formation of high-valent iron species. Acting as redox mediators, the phenolic hydroxyl groups can promote the production of Fe(IV) and Fe(V) through the electron-shuttle mechanism with Fe(VI). Recent studies have shown that oxidants (e.g., PMS, H_2O_2, and periodic acid) combined with Fe(VI) can induce the formation of highly reactive Fe(IV) and Fe(V) intermediates [27]. Scavenging experiments were performed to verify whether the active species play a role in the degradation of contam-

inants [29]. Methyl phenyl sulfoxide (PMSO) has been widely employed to confirm the formation of high-valent Fe because it can react with Fe(V)/Fe(IV) to form methyl phenyl sulfone ($PMSO_2$) as a diagnostic product [30]. PMSO was utilized to identify the roles of Fe(V)/Fe(IV) species in the removal of sulfamethoxazole (SMX) [31] and polycyclic aromatic hydrocarbons [32] in the Fe(VI)-PMS system. The selective conversion of PMSO into $PMSO_2$ demonstrates the formation of high-valent Fe species (Fe(V)/Fe(IV)) [33]. To quench the reactive species, ethylene diamine tetraacetic acid was used as a photogenerated hole quench agent, and tert-butanol (TBA) was added to eliminate •OH. Sodium azide is a widely used scavenger of $^1O_2$, while p-benzoquinone was used to detect O_2•$^-$ [33]. Benzoic acid and methanol (MeOH) were utilized to quench SO_4•$^-$ and •OH and establish their effects on the removal of SMX in the Fe(VI)/PMS process [31,34]. In the quenching experiment, the results indicated that the photogenerated electrons and •OH radicals play important roles in the degradation of dimethyl phthalate (DMP) [35]. In the Fe(VI) and Fe(VI)/percarbonate systems, PMSO, ethanol (EtOH), and benzoic acid were employed as scavengers to determine the changes in the reactive species after the addition of percarbonate [34]. Radical quenching experiments with EtOH and TBA were conducted to distinguish the contribution of •OH and SO_4•$^-$ to the removal of bisphenol A (BPA) in the reaction system [36].

2.1. Photocatalysis

Fe(VI) has a relatively high redox potential, and its reduction products are nontoxic Fe oxides [37]. Fe(VI) can enhance photoreaction processes significantly (Figure 1, Table 1), which is due to the high reactivity between Fe(VI) and the conduction band electrons e^- ($k = 2.0 \times 10^{10}$ $M^{-1}s^{-1}$) in photocatalytic oxidation systems [38]. This prevents the recombination of e^--h^+ pairs, which improves the quantum efficiency of the UV-TiO_2-Fe(VI) system [35]. The hydrolysis of Fe(VI) can be essentially activated by ultraviolet light, which promotes the formation of Fe(IV) and H_2O_2 and particularly enhances the generation rate of O_2•$^-$ and •OH [39]. DMP was barely degraded by Fe(VI), whereas UV-TiO_2-Fe(VI) oxidation showed a 3–11 times higher removal efficiency than the oxidation of Fe(VI) alone. The participation of Fe(VI) in the photoreaction also led to an increase of approximately 83.8% in the degradation rate compared to that in the UV-TiO_2 process alone [35]. The degradation of BPA was similarly enhanced in the order of UV-TiO_2 < Fe(VI) < UV-TiO_2-Fe(VI) based on the scavenging of e^- by Fe(VI) [22]. The Fe(VI)-TiO_2-UV system showed high DMP degradation under UV irradiation, because the electron scavenging by Fe(VI) greatly reduced the recombination of the e^- and h^+ [40]. The Fe(VI) concentration decreased rapidly in the presence of a TiO_2 suspension under UV light [41]. The influence of light wavelength on the SMX degradation efficiency in the UVA-Fe(VI)-PMS process was also investigated [42]. Compared to the reaction in the dark, SMX removal increased with the introduction of light at all the examined wavelengths. Therefore, Fe(VI) may affect the photocatalytic oxidation reaction by absorbing light.

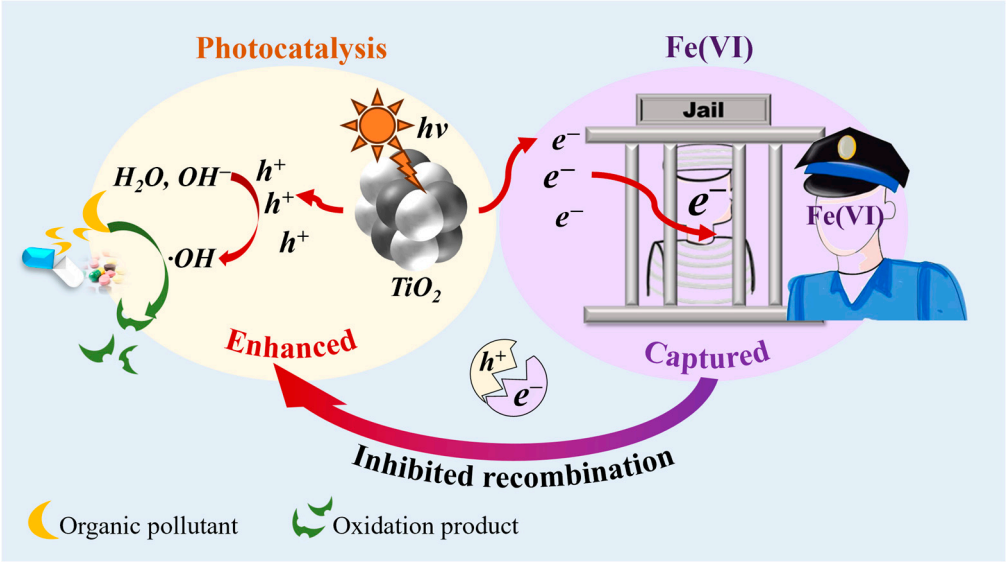


Figure 1. Enhanced mechanism of Fe(VI) in photocatalysis.

Table 1. Removal of organic pollutants in ferrate-AOP systems with the main species of Fe(VI), Fe(V), and Fe(IV).

Experimental System	Experimental Condition	Active Specie	Adjustments	Pollutant	Enhancement Effect	Reference
UV-TiO_2-Fe(VI)	[Fe(VI)]: 50.0 μM; [TiO_2]: 0.5 g/L; light intensity: 0.15 mW/cm^2 at 254 nm; pH 9.0	h^+ and OH	pH	Sulfadiazine/ Sulfamerazine/ Sulfamethoxazole: 20.0 μM	UV-TiO_2-Fe(VI): 89.2%, 83.4%, 82.0%; UV-TiO_2: 71.3%, 72.7%, 76.0%; Fe(VI): 65.2%, 66.0%, 71.9%	[43]
Fe(VI)-UV-TiO_2	[Fe(VI)]: 80.0 μM; [TiO_2]: 2.0 g/L; light intensity: 4.0 mW/cm^2 at 340–420 nm; pH 6.0	Fe(V) and Fe(IV)	pH	Microcystin-LR: 1.0–2.0 mg/L	Fe(VI)-UV-TiO_2: 100.0%; UV-TiO_2: 63.0%; Fe(VI): 54.0%	[44]
Fe(VI)-UVA-light-emitting diode (LED)	[Fe(VI)]: 75.0 μM; LED bulb: 3.0 W; UVA: 37.0 mW/cm^2; pH 8.0	Fe(V) and Fe(IV)	pH	Sulfamethoxazole: 5.0 μM	Fe(VI)-UVA-LED: Reacting 2.6−7.2-fold faster than for Fe(VI)	[45]
UV-TiO_2-Fe(VI)	[Fe(VI)]: 30.0 mg/L; [TiO_2]: 0.05 g/L mg/L; light intensity: 9 W at 365 nm; pH 9.0	h^+ and•OH	pH and oxidant dosage	Dimethyl phthalate: 0.3 mg/L	UV-TiO_2-Fe(VI): 95.2%; UV-TiO_2: 51.8%; Fe(VI): 23.5%	[35]
Fe(VI)-UV-TiO_2	[Fe(VI)]: 9.0 mg/L; [TiO_2]: 40.0 mg/L; light intensity: 0.4 mW/cm^2 at 365 nm; pH 9.0	Holes, OH, and Fe(V)	Oxidant dosage	Dimethyl phthalate: 11.6 mg/L	Fe(VI)-UV-TiO_2: 83.0%; UV-TiO_2: 68.0%; Fe(VI): negligible	[41]

Table 1. *Cont.*

Experimental System	Experimental Condition	Active Specie	Adjustments	Pollutant	Enhancement Effect	Reference
Fe(VI)-Visible light-g-C_3N_4	[Fe(VI)]: 100.0 μM; [g-C_3N_4]: 50.0 mg/L; visible light; pH 9.0	Fe(V) and Fe(IV)	Oxidant dosage	Carbamazepine: 5.0 μM	Fe(VI)-Visible light-g-C_3N_4: 100.0%; Visible light-g-C_3N_4: 41.0%; Fe(VI)-Visible light: 38.0%	[33]
Fe(VI)-CaO_2	[Fe(VI)]: 50.0 μM; [CaO_2]: 50.0 μM; pH 8.0	Fe(V) and Fe(IV)	Oxidant dosage	Sulfamethoxazole: 5.0 μM	Fe(VI)-CaO_2: 82.7%; CaO_2: negligible; Fe(VI): 35.4%	[46]
Fe(VI)-H_2O_2	[Fe(VI)]: 50.0 μM; [H_2O_2]: 0–30.0 μM; pH 8.0	Fe(V) and Fe(IV)	Oxidant dosage	Caffeine: 5.0 mM	k_{app} between caffeine and Fe(VI): 12.8 to 171.8 $M^{-1}s^{-1}$ with H_2O_2 from 0 to 30.0 μM	[47]
Fe(VI)-H_2O_2	[Fe(VI)]: 50.0 μM; [H_2O_2]: 70.0 μM; pH 7.0–9.0	Fe(V) and Fe(IV)	Oxidant dosage	Sulfamethoxazole: 5.0 μM	Fe(VI)-H_2O_2: 78.0%; H_2O_2: negligible; Fe(VI): 35.0%	[48]
Fe(VI)-H_2O_2	[Fe(VI)]: 250.0 μM; [H_2O_2]: 2.5 mM; pH 8.0	Fe(V) and Fe(IV)	Oxidant dosage	Bisphenol A: 50.0 μg/L	Fe(VI)-H_2O_2: 97.7%; H_2O_2: 23.5%; Fe(VI): 85.5%	[49]
Fe(VI)-UV	[Fe(VI)]: 0.2 mM; light intensity: 26.0 μW/cm^2 at 254 nm; pH 7.0	O_2•$^-$,•OH, Fe(V) and Fe(IV)	Dosing pattern	Lake water	Fe(VI)-UV: UV_{254} removal increased; TOC removal increased than Fe(VI)	[40]

Fe(V) and Fe(IV) are high-valent Fe species with selective oxidation behaviors that differ from those of free radicals [50]. Fe(V) and Fe(IV) can be produced from Fe(VI) through one- and two-electron transfer, where electrons can be provided by pollutants, H_2O, H_2O_2, and photocatalysis-generated e^- [27,33]. The observed first-order rate constants of Fe(V) and Fe(IV) with pollutants are approximately 10^3 and 10^5 times that of Fe(VI), respectively [51]. Therefore, the generation of Fe(V) and Fe(IV) usually contributes to a greater removal efficiency of organic pollutants. These ferrate-AOP systems, based on the generation of Fe(V) and Fe(IV), generally show advantages such as low toxicity, low generation of disinfection by-products, and high interference resistance to natural organic matter. In certain Fe(VI) photocatalytic systems, Fe(V) and Fe(IV) produced by the combination of Fe(VI) with photocatalyzed electrons dominate the oxidation of organic pollutants (Figure 2). Scavenging tests and electron paramagnetic resonance analysis were conducted by adding quenching agents of TBA and MeOH and trapping agents of 5,5-dimethyl-1-pyrroline-N-oxide (DMPO). The results revealed a small contribution of free radicals, and Fe(V) and Fe(IV) were determined to play a primary role in the degradation of pollutants [45].

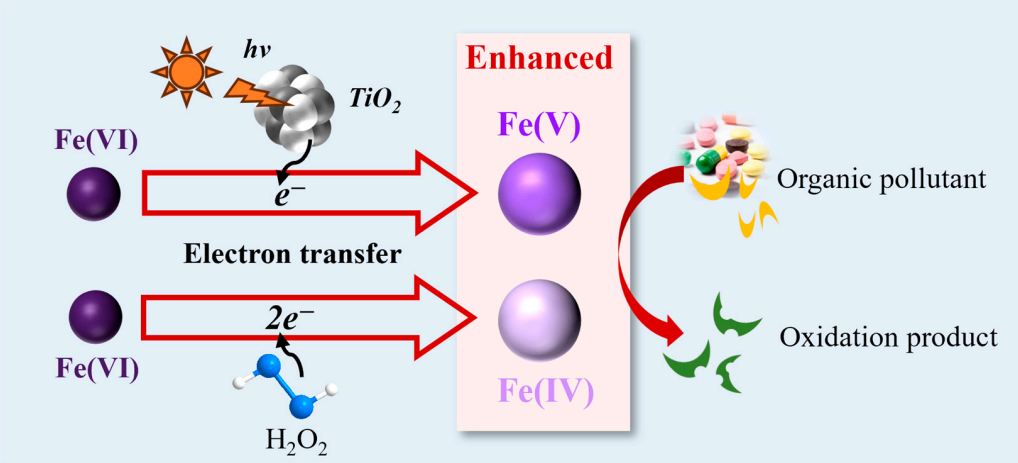


Figure 2. Enhanced mechanism based on Fe(V) and Fe(IV) oxidation.

Fe(V) attacked the alkyl chain of DMP instead of the aromatic rings, following a different degradation path than the •OH oxidation pathway [41]. Probing the reaction with PMSO revealed that Fe(V) and Fe(IV), which were produced in the oxygen-doped $ZnIn_2S_4$ nanosheet-visible light-Fe(VI) combined system, were responsible for the high removal of trimethoprim [52]. MeOH and TBA had negligible effects on SMX removal, indicating that •OH radicals contributed little to SMX oxidation [45]. There was no DMPO-HO• adduct signal observed, suggesting that •OH played a negligible role in the Fe(VI)-UVA-LED process [45]. PMSO can be oxidized to phenyl methyl sulfone ($PMSO_2$) specifically by high-valence Fe species [31]. The ratio of produced $PMSO_2$/reduced PMSO was close to 100% in the photocatalytic Fe(VI)-visible light-g-C_3N_4 systems, indicating that Fe(V) and Fe(IV) were the dominant reactive oxidation species in the degradation of micropollutants [33]. The •OH generation pathway from ferrate self-decay is inhibited by the remarkable oxidation between Fe(VI) and organic pollutants. The Fe(V) and Fe(IV) generated from Fe(VI) facilitate several orders of reactivity with organic pollutants, reducing the self-decay of Fe(V) and Fe(IV) in water [33].

2.2. Fenton-like Reaction

Electron transfer efficiency in Fe(VI)-H_2O_2 systems is strongly dependent on pH. Under alkaline conditions, H_2O_2 promotes the decomposition of Fe(VI), resulting in highly oxidizing Fe(IV) [53]. Under acidic conditions, Fe(II) and H_2O_2 react to form a Fenton system through a series of chain reactions. The •OH produced is also actively involved in the oxidation of pollutants [54]. Fe(VI) can be reduced to Fe(IV) by a two-electron transfer with H_2O_2 (Figure 2) and subsequently to Fe(II). Fe(VI) has much higher reactivity with H_2O_2 than with H_2O; therefore, the generation of Fe(IV) is enhanced in the Fe(VI)–H_2O_2 system compared to that in individual Fe(VI) [47]. The conversion tendency of Fe(IV) into Fe(II) is high with H_2O_2 ($k = 10^4$ $M^{-1}s^{-1}$). The Fe(II) thus generated reacts further with Fe(VI) to produce Fe(V) ($k = 10^7$ $M^{-1}s^{-1}$) [55]. This explains the higher concentrations of Fe(V) and Fe(IV) for the ferrate-H_2O_2 system, which is consistent with the observed increase in pollutant removal from 35.0 to 78.0% for SMX [48].

Radical-scavenging experiments demonstrated the dominant roles of Fe(V) and Fe(IV) in the degradation of organic pollutants. SMX removal by ferrate-H_2O_2 is barely affected by the addition of TBA ($k_{•OH/TBA}$ = 3.8–7.6 × 10^8 M^{-1} s^{-1}) and MeOH ($k_{•OH\ /MeOH}$ = 9.7 × 10^8 $M^{-1}s^{-1}$), which rules out the contribution of •OH radicals. The 100% yield of $PMSO_2$ confirmed the dominant contribution of high-valence Fe species. Moreover, the contribution of Fe(VI) was ruled out by the strong inhibitory effect of SMX

removal with PMSO, as Fe(VI) has much higher reactivity with SMX than with PMSO. Thus, the main contributions of Fe(V) and Fe(IV) were confirmed [48]. The same phenomenon was observed for SMX oxidation in the ferrate-CaO_2 system, where CaO_2 was used as a sustainable resource for H_2O_2 [46]. The oxidation pathway of BPA in the ferrate-H_2O_2 system differs significantly from that of the H_2O_2 process but is highly similar to pure ferrate oxidation, indicating that the oxidation can be attributed to Fe(V) and Fe(IV) [49].

As the dosage of H_2O_2 ranged from 0 to 30 μM, the removal rates of caffeine and carbamazepine (CBZ) in the ferrate-H_2O_2 system increased [47]. These findings confirmed that the addition of H_2O_2 promoted the decomposition of Fe(VI) and the generation of Fe(V) and Fe(IV) [47]. The enhanced Fe(V) and Fe(IV) production promoted pollutant removal significantly. At pH 8, the SMX removal rate was 1.2 and 1.3 times higher by the Fe(VI)-H_2O_2 and Fe(VI)-CaO_2 systems, respectively, when compared to the removal rate with Fe(VI) alone [46,48]. Similarly, BPA removal was strengthened in the Fe(VI)-H_2O_2 system, with an 11.1% increase in the removal rate when H_2O_2 was added to Fe(VI) [49]. Peracetic acid (PAA) and percarbonate can also act as suppliers of H_2O_2 to enhance the ferrate oxidation process, contributing to the enhanced degradation of CBZ [56] and an increase in fatty acid production via sludge pretreatment [57].

Fe(VI) reduction products, including Fe(III) and Fe(II) and Fe oxides, can be used as alternative Fe catalysts for Fenton-like reactions [58]. Unlike the traditional Fenton reaction, ferrite-based Fenton-like reactions have several advantages, such as low pH dependence and a lower dosage of oxidants [58]. Ferrate-based Fenton-like reactions play an important role in •OH production from ex situ H_2O_2 under the catalysis of Fe(III) and Fe(II) from Fe(VI), which is a more common sequence than dosing of Fe(VI) followed by H_2O_2 [59,60]. Fe(VI) pretreatment for organic dyes was conducted for 30 min, which caused most of the Fe(VI) to decompose into Fe(III) and Fe(II) species [60]. Ex situ H_2O_2 was then added. The significant increase in the color-reduction rate after H_2O_2 addition indicated the activation of a Fenton-like reaction [60]. The degradation rate of phenanthrene was 10.4% greater than that when only Fe(VI) was added [59]. The degradation rate of DMP was controlled by the concentration of •OH, indicating that a Fenton-like reaction activated by Fe(III) and Fe(II) contributed to oxidation [58].

2.3. O_3

Secondary wastewater treatment using Fe(VI) and ozonation has a synergistic oxidation effect due to the Fe(III)/Fe(II) and FeOOH/Fe_2O_3 particles. This enhancement was found to increase dissolved organic carbon by 14.9% and UV_{254} removal by 29.0% [19]. This combined system can also be used for the removal of tetrabromobisphenol A, with the complete removal of contaminants and a higher mineralization rate [61]. The SMX and diclofenac sodium can also be removed efficiently by the ozone/Fe(VI) process. With the increase in Fe(VI) dosage or ozone concentration, the degradation rate of SMX and diclofenac sodium was significantly accelerated, reaching 77.0% and 82.7% [62].

As shown in Table 2, the main enhancing effect stems from the catalytic effect of the Fe(VI) reduction products on ozonation, partly because of the production of high-valent Fe formed from the oxidation of Fe(III)/Fe(II) by ozone [19,61]. On the one hand, Fe(VI) could activate O_3 to produce •OH; on the other hand, O_3 also helps regenerate Fe(VI) [63]. The decomposition of O_3 and Fe(VI) occurs simultaneously, and the Fe(III)/Fe(II) ions and FeOOH/Fe_2O_3 particles further promote the decomposition of O_3. The decomposition of Fe(VI) was reported to produce Fe nanostructures with a γ-FeOOH shell and a γ-Fe_2O_3 core [64], with the dissociation of water molecules on its surface leading to hydroxylation, which further aids the bonding between ozone and surface -OH to produce •OH [19].

Table 2. Removal of organic pollutants in ferrate-AOP systems with the main species of Fe(III) and Fe(II).

Experimental System	Experimental Condition	Active Specie	Adjustments	Pollutant	Enhancement Effect	Reference
Fe(VI)-PMS	[Fe(VI)]: 0.05 mM; [PMS]: 0.05 mM; pH 5.2	$SO_4\bullet^-$ and •OH	pH	Sulfamethoxazole: 0.1 mM	Fe(VI)-PMS: 55.5% in 30 min; PMS: negligible; Fe(VI): 20.0%	[65]
Fe(VI)-PMS	[Fe(VI)]: 2.5 mM; [PMS]: 5.0 mM; pH 6.0	$SO_4\bullet^-$ and •OH	Oxidant dosage	Atrazine: 46.5 μM	Fe(VI)-PMS: 81.5% in 60 min; PMS: negligible; Fe(VI): 11.7%	[66]
Fe(VI)-PMS	[Fe(VI)]: 100.0 μM; [PMS]: 500.0 μM; pH 6.0	$SO_4\bullet^-$ and •OH	Oxidant dosage	Diclofenac: 5.0 μM	Fe(VI)-PMS: 93.5% in 15 min; PMS: negligible; Fe(VI): 42.2%	[42]
Fe(VI)-PMS	[Fe(VI)]: 30.0 μM; [PMS]: 30.0 μM; pH 7.0	$SO_4\bullet^-$ and •OH	Oxidant dosage	Enrofloxacin/ marbofloxacin/ ofloxacin: 30.0 μM	Fe(VI)-PMS: 48.0%, 55.0% and 59.0%; PMS: 19.0%, 21.0% and 18.0%; Fe(VI): 14.0%, 10.0% and 13.0%	[67]
Fe(VI)-PMS	[Fe(VI)]: 10.0 mg/L; [PMS]: 2.0 mg/L; pH 7.0	$SO_4\bullet^-$ and •OH	Oxidant dosage	Chlorpyrifos: 2.0 mg/L	Fe(VI)-PMS: 94.8% in 90 min; PMS: 56.5%; Fe(VI): 83.0%	[68]
Fe(VI)-PDS/PMS	[Fe(VI)]: 0.25 mM; [PDS]: 0.5 mM; [PMS]: 0.5 mM; pH 7.0	$SO_4\bullet^-$, $^1O_2$, •OH, Fe(V) and Fe(IV)	pH and Oxidant dosage	Ibuprofen: 20 μM	Fe(VI)-PDS: 31.1%; Fe(VI)-PMS: 92.8%	[69]
Fe(VI)-PMS	[Fe(VI)]: 50 mM; [PMS]: 200 mM; pH 7.0	$SO_4\bullet^-$, Fe(V) and Fe(IV)	pH and Oxidant dosage	Sulfamethoxazole: 10 μM	Fe(VI)-PMS: >80% in 15 min	[70]
Fe(VI)-PMS-light	[Fe(VI)]: 1.0 mg/L; [PMS]: 5.0 mg/L; Solar irradiance: 550 W/m^2; T: 35.0 °C; pH 6.5	$SO_4\bullet^-$ and •OH	Oxidant dosage	Sulfamethoxazole: 0.1 mg/L	Fe(VI)-PMS-light: 70.0% in 60 min; PMS-light: 20.0%	[71]
Fe(VI)-O_3	[Fe(VI)]: 300.0 μM; [O_3]: 13.5 mg/L; pH 7.0	•OH	Dosing pattern	Dissolved organic carbon (DOC): 8.4 mg/L; UV_{254}: 0.174	Fe(VI)-O_3: 53.0% (DOC); Ozonation: 23.0% (DOC); Fe(VI): 21.0% (DOC); Fe(VI)-O_3: 70.0% (UV_{254}); Ozonation: 44.0% (UV_{254}); Fe(VI): 35.0% (UV_{254})	[19]

Table 2. *Cont.*

Experimental System	Experimental Condition	Active Specie	Adjustments	Pollutant	Enhancement Effect	Reference
Fe(VI)-O_3	[Fe(VI)]: 150.0 μM; [O_3]: 10.0 mg/L; O_3: 100.0 mL/min; pH 6.3–6.4	•OH	Dosing pattern	DOC: 7.5 mg/L; UV_{254}: 0.15	Fe(VI)-O_3: 70.5% (DOC), 80.5% (UV_{254}); O_3: 26.7% (DOC), 60.0% (UV_{254})	[72]
Fe(VI)-O_3	[Fe(VI)]: 0.5 μM; [O_3]: 0.5 μM; pH 7.0	•OH	Dosing pattern	Tetrabromobisphenol A:1.8 μM	Fe(VI)-O_3: 68.9% in 1 min Ozonation: 11.7%; Fe(VI): 32.0%	[61]
Fe(VI)-O_3	[Fe(VI)]: 25.0 μM; [O_3]: 52 μM; pH 5–9	•OH	pH	Sulfamethoxazole/ diclofenac sodium: 20 μM	Fe(VI)-O_3: 98.4% and 94.3%; O_3: slightly enhanced than the Fe(VI) alone process; Fe(VI): 65.3% and 85.5%	[62]
Fe(VI)-O_3	[Fe(VI)]: 0.2 mM; [O_3]: 15.1 mg/L; pH 5–9	•OH	pH	Atrazine: 5 mg/L	Fe(VI)-O_3: 90.1% in 18 min	[63]
Fe(VI)-O_3-ceramic membrane	[Fe(VI)]: 150.0 μM; [O_3]: 10 mg/L; filtration flux: 90 L/(m^2·h); pH 6.0–6.4	•OH	Dosing pattern	DOC: 6.0 mg/L; UV_{254}: 0.1; Protein: 3.0 mg/L	Fouling transmembrane pressure decreased 96.7% with Fe(VI)-O_3	[73]
Fe(VI)-PDS	[Fe(VI)]: 90.0 μM; [PDS]: 90.0 μM; pH 4.0	SO_4•$^-$ and •OH	Reducing and complexing additives	Ciprofloxacin: 30.0 μM	Fe(VI)-PDS: 72.6% in 15 min; PDS: negligible; Fe(VI): 54.2%	[74]

2.4. Persulfate

Persulfate, including PMS and PDS, have received increasing attention as AOP precursors due to their advantages of low cost, stable physicochemical properties, and high redox potential [75]. Moreover, sulfate radicals (SO_4•$^-$) from PMS or PDS activation show higher stability and more powerful oxidation ability compared to •OH [76]. Fe-based catalysts are commonly used as effective and environment-friendly activators of PMS and PDS [77].

Fe(II) ions are commonly used as homogeneous activators with higher reactivity with PMS and PDS to produce SO_4•$^-$ radicals (Figure 3) [3]. The amount of Fe(II) ions in the Fe(VI)-PMS system first increased to 9 μM at 3 min and then decreased continually to less than 2 μM at 15 min, which is consistent with the degradation curve of PMS and diclofenac, where 93.5% of diclofenac was removed within 15 min [42]. A similar trend in Fe(II) ion concentration was observed in the Fe(VI)-PMS system for atrazine degradation, indicating the involvement of Fe(II) ions in the activation of PMS for contaminant degradation [66]. An *o*-dichlorobenzene removal rate of 76.5% was achieved using Fe(VI)-PMS, and the removal efficiency increased to 86.4% when FeS was used as the catalyst. The main contribution of FeS was the provision of additional Fe(II) ions for PMS activation [78]. High SMX degradation in Fe(VI)-PMS system was due to the presence of Fe^{3+} ions from the rapid decomposition of Fe(VI), which increases the rate of production of SO_4•$^-$ [70].

Heterogeneous materials such as Fe_2O_3 have been used for PMS activation in rhodamine B degradation, showing a 1.5-fold increase in the decolorization rate compared with the reaction with no activator [79]. Fe(VI) residual particles (γ-Fe_2O_3) were separated and shown to have catalytic effects on PMS, causing a 58.6% degradation of atrazine [66]. Compared with the low removal of 31.1% in Fe(VI)–PDS, the Fe(VI)–PMS system provided a synergistic effect for ibuprofen removal of 92.8% [69]. Superior to the use of ferric and polymeric coagulant individually, Fe(II)/PMS treatment was utilized to promote the removal of alkali lignin in wastewater. At the optimal dose of 2.4 mM for Fe(II) and 7.8 mM for PMS, the removal efficiency of alkali lignin (2 g/L) can reach 99% [80].

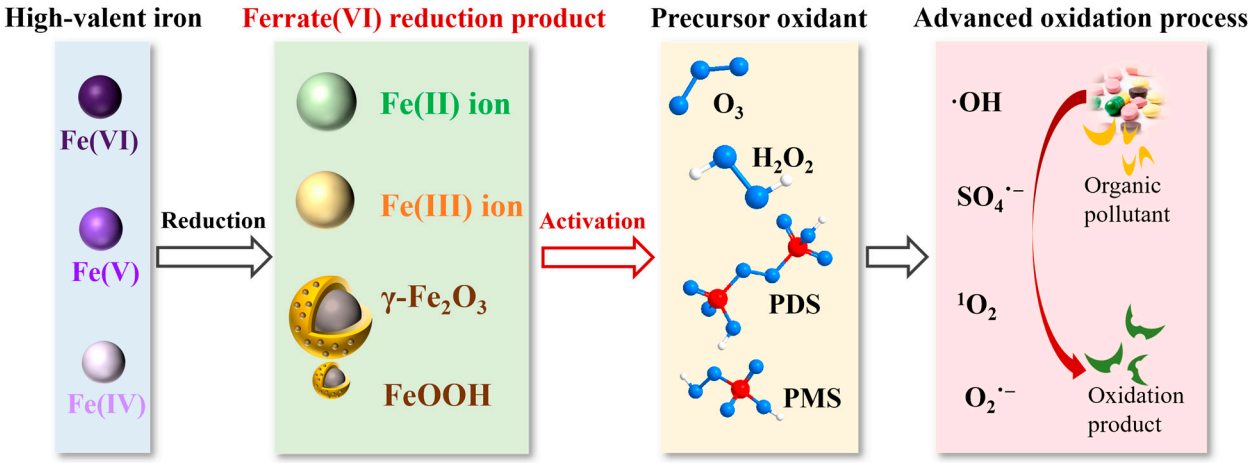


Figure 3. Contributions of Fe(III) and Fe(II) to ferrate-based AOPs and their applications.

The catalytic effect of Fe(III) and Fe(II) on the formation of radicals in the Fe(VI)-persulfate systems was revealed by quenching experiments in which $SO_4\bullet^-$ and •OH played a dominant role in the removal of organic pollutants [81]. The inhibition rate of diclofenac degradation by either MeOH or tetrabromobisphenol A was more than 50%, and the same suppression effect was observed for atrazine degradation in a similar Fe(VI)-PMS system at pH 6 [42,66] and ciprofloxacin (CIP) removal at pH 4 in the Fe(VI)-PDS system [74]. Fe(III) and Fe(II) can react with PMS or PDS to form $SO_4\bullet^-$, $SO_5\bullet^-$, and $S_2O_8\bullet^-$ [27,82,83]. Fe(II) showed a reaction constant of $k = 3.0 \times 10^4$ $M^{-1}s^{-1}$ with HSO_5^-, whereas Fe(III) presented limited catalytic reactivity [84].

3. Adjustment of the Fe Species in Ferrate-Based AOP Systems

Ferrate can play the role of (1) oxidant, (2) activator, or (3) electron scavenger in ferrite-based AOP combined systems, depending on the AOP conducted, solution pH, dosage strategy of chemicals, and chemical structure of the contaminants. These roles are not isolated from each other, and Fe(VI) can play two or more roles in one system, causing a synergistic effect with AOPs. By adjusting certain factors, the function of ferrate can be controlled and, more importantly, the total efficiency of ferrite-based AOP systems can be improved (Table 1).

3.1. pH

Solution pH is a key factor that determines the oxidation efficiency of ferrate-based AOP systems [15]. It generally influences the oxidation process in four ways (Figure 4): (1) It determines the concentration and speciation of different valences of iron [65]. (2) It affects the generation and oxidation capability of free radicals [78,85]. (3) It influences the pollutant structure [31]. (4) It influences the oxidant species [60,66]. Among the four

methods, the influence of pH on Fe(VI) is the most significant because of its important role as an oxidant and activator.

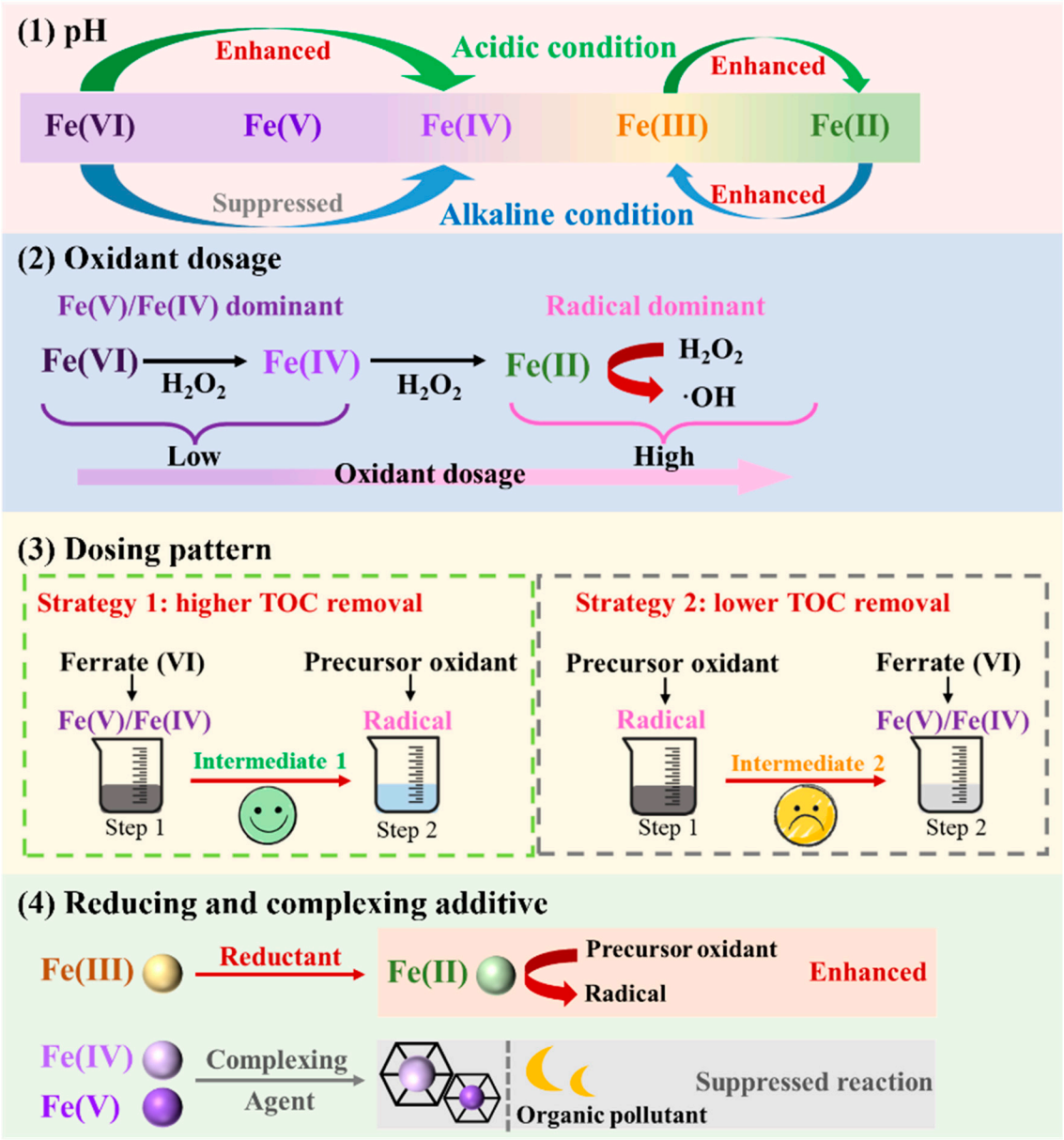


Figure 4. Adjusting the Fe species in ferrate-based AOPs.

Controlling the pH can determine the molecular structure of high-valent Fe species and further influence the oxidation system, owing to the different decomposition pathways of Fe(VI) under various conditions [18]. Fe(VI) is distributed into four different chemical structures depending on the pH of the solution. At an acidic and neutral pH, the dominant $HFeO_4^-$ forms $Fe^{VI}_2O_7^{2-}$ via O–O coupling to produce $Fe^{IV}_2O_6^{2-}$, whereas under base conditions, H_2O molecules attack FeO_4^{2-} to form an O–O bond, followed by the release of Fe(IV). This also leads to different ferrate decomposition rates, which decrease significantly from 4×10^{-3} at pH 7 to below 1×10^{-4} at pH 9 and generally remain stable at pH 9–12 [86]. The self-decomposition of Fe(VI) is significantly dependent on pH. The lower pH increases the oxidizing capacity of Fe(VI), but the decomposition rate becomes faster [27]. The active iron produced has a short service life, and the final decomposition product is Fe(II)/Fe(III) [53]. Therefore, an optimized pH can be used to adjust the Fe species and generate high reaction rates in the AOPs [87].

When high-valent Fe species are the dominant electron acceptors, such as when acting as electron scavengers in UV-TiO_2-Fe(VI) and as the dominant oxidant in ferrate-H_2O_2, the balance between the oxidation capability and stabilization usually lies near pH 7. pH 7 was found to be more effective for the removal of sulfonamides in the UV-TiO_2-ferrate system [43]. A neutral pH is also suitable for SMX degradation in the Fe(VI)-UVA-LED system, with removal efficiencies of 98% and 90% within 2 min at pH 7 and 8, respectively [45]. Increasing the pH enhanced microcystin-LR removal from 65% at pH 2 to 100% at pH 6 [44].

When Fe(III)/Fe(II) is used as an activator for the persulfate and Fenton reactions, acidic conditions are preferred because of the higher Fe^{2+} ion concentrations in this pH range, resulting in a higher activation efficiency. In Fe(VI)-PMS at pH 3.2–11.2, the generation of Fe^{2+} ions was rapid in the first few minutes and then decreased continually during the reaction [65]. The highest concentration of ferrous ions was generated at pH 3.2, which was consistent with the best SMX removal performance [65]. The degradation of SMX decreased at pH from 3 to 11, with the highest removal rate in a Fe(VI)-PMS system without photolysis occurring at pH 3 [31].

3.2. Oxidant Dosage

The dose of H_2O_2 influences the Fe species through electron transfer between H_2O_2 and ferrate. When 50 μM CaO_2 was used as a slow H_2O_2-releasing material, the yield of $PMSO_2$ in the ferrate-CaO_2 system was nearly 100%, indicating that a low H_2O_2 dosage enhanced oxidation by accelerating the production of Fe(V) and Fe(IV) [46]. While a high H_2O_2 dosage system may initially generate Fe(V) and Fe(IV), a Fenton-like reaction occurs in the later reaction process, catalyzed by Fe(III)/Fe(II) generated from Fe(VI) decay [58]. However, information on the reactive oxidation species in ferrate-H_2O_2 at high H_2O_2 dosages is required. An increase in the H_2O_2 dosage within a certain range is beneficial for the degradation of contaminants; however, an excessive dosage of H_2O_2 reduces the oxidation efficiency. At the initial concentration of Fe(VI) of 50 μM, the degradation of PMSO increased as the H_2O_2 dosage increased from 0 to 30 μM [47]. Similar phenomena were observed for the degradation of SMX, dimethyl phthalate, and BPA [48,49,58]. However, a continual increase in the H_2O_2 dosage inhibits oxidation due to the competition between Fe(V)/Fe(IV) or •OH and H_2O_2 and the contaminants [48,60,85].

The enhanced oxidation effect of persulfate and ferrate is achieved by the activation of persulfate by Fe^{2+}, Fe^{3+}, γ-FeOOH, and γ-Fe_2O_3 from Fe(VI) decomposition. An insufficient dosage of persulfate leads to wasted Fe(VI) decomposition products, whereas an excess dose of persulfate leads to a quenching effect and competition for radicals [88]. With an increase in the PMS dosage from 50 to 200 μM, the percentage of PMSO oxidized by free radicals increased from 5% to 20%, indicating that the utilization of Fe(II) and Fe(III) by PMS was enhanced [31]. The degradation removal of ATZ increased from 25% to 100% when the molar ratio of Fe(VI) to PMS was increased from 6:5 to 10:1 [66], which is consistent with observations of the degradation of chlorpyrifos, which showed that when the molar ratio was increased from 2:1 to 10:1, the removal efficiency increased from 83.0% to 97.5% [68]. A similar phenomenon was observed in the degradation of diclofenac [42]. The increase in the PMS dosage also enhanced degradation due to the enhanced production of sulfate radicals [67,68]. However, upon increasing the PMS dosage, diclofenac oxidation was inhibited, decreasing to 85% [42]. Response surface methodology was used to analyze the degradation of SMX, and it was found that the dosage of Fe(VI) had a positive effect on SMX removal [89].

3.3. Dosing Pattern

The dosing strategy of Fe(VI) and precursor oxidants influences the degradation efficiency of pollutants because of the interactions between Fe(III)/Fe(II) and the precursor oxidants. The UV_{254} removal efficiency was higher when the treatment involved Fe(VI) followed by ozone than when ozone was followed by Fe(VI) because at a pH of approximately 7.5, the intermediates of the ozone (E_0 = 2.07 V) treatment were harder to mineralize using Fe(VI) (E_0 = 0.72 V), and the catalytic effect of Fe(III)/Fe(II) on ozone was hindered by the relatively low ozone concentration when Fe(VI) was added [19]. For the same reason, in another combined Fe(VI)-O_3 process, ozone pre-oxidation also inhibited the degradation of tetrabromobisphenol A [61]. The Fe(VI)-ozone system achieved 76.0% and 76.7% removal efficiencies, while the ozone-Fe(VI) system only yielded 49.4% and 54.8% removal for SMX and DCF. The ozone-Fe(VI) system exhibited limited removal efficiency due to rapid ozone depletion by organics and subsequent competitive consumption of Fe(VI) by degradation intermediates [62]. Based on the utilization of Fe(II) in a Fenton-like reaction, the degradation efficiency when H_2O_2 was added at 30 min was the lowest among the cases of the simultaneous addition of the two oxidants and the addition of H_2O_2 at 10 min, owing to the decreasing concentration of Fe(II) with time [85].

The stepwise addition of Fe(VI) slowed the oxidation of SMX when the intermediates competed for radicals, thereby promoting TOC removal [65]. The stepwise addition of PMS caused a radical-scavenging effect via the reaction between the Fe^{2+} and low concentrations of radicals [65]. In a similar case of the TOC removal of CBZ, applying ^{60}Co radiation followed by the Fe(VI) process increased the removal rate to 1.8 times the sum of the removal rates of single treatments, which could have resulted from formic, acetic, and oxalic acids generated by the radiation being decomposed by Fe(VI) [90].

3.4. Reducing and Complexing Additives

The conversion between Fe^{2+} and Fe^{3+} is a key factor in controlling the catalytic efficacy of PDS and PMS because Fe^{2+} has a higher catalytic efficiency [36]. Hydroxylamine [74], solar light [71], and sulfites [91] can promote the conversion of Fe^{3+} into Fe^{2+}. The addition of hydroxylamine to the Fe(VI)-PDS system to increase the concentration of Fe^{2+} increased the CIP removal efficiency by approximately 20% compared with that in normal Fe(VI)-PDS systems. Reducing agents such as sodium thiosulfate and ascorbic acid have also been reported to enhance CIP degradation in Fe(VI)-PDS systems [74]. Ex situ Fe^{2+} can also be added to enhance the production of Fe(V)/Fe(IV) from Fe(VI) and simultaneously activate PMS [78]. In the Fe(VI)/sulfur reducing agent system, over 90% of PMSO was converted to $PMSO_2$ at pH 8–10 [92]. At a sulfite concentration of 10 μM, the removal ratio of PMSO was 37.5%, and the molar ratio of $PMSO_2$ and PMSO was 95.5%, suggesting the presence of Fe(IV) and Fe(V) [45].

Some complexing agents can promote the electron transfer efficiency between oxidants and pollutants. PAA is an oxidant that functions similarly to H_2O_2 and decomposes into H_2O_2 in water. An additional promoting effect on the removal efficiency was observed by comparing the Fe(VI)-PAA system with Fe(VI)-H_2O_2 when the concentration of H_2O_2 was equivalent to that produced in PAA at pH 9 when treated with CBZ [56]. At pH 7 and 8, the combination of PAA with ferrate(VI) demonstrated significantly enhanced CBZ removal efficiency compared to ferrate(VI) alone [26]. Similarly, the addition of PAA to the ferrate(VI) system enabled rapid CBZ removal, reaching 90% efficiency within 1 min [93]. It was assumed that the PAA complexed with Fe(V)/Fe(IV) and that the complex was more oxidative than the common hydroxide Fe complex. The addition of quinone to ferrate systems prominently improves the treatment performance by activating the decomposition of ferrate into Fe(V) and Fe(IV) [21].

4. Effect of Wastewater Composition and Compatibility with Traditional Treatment Methods

Natural organic matter can enhance or inhibit the efficiency of ferrate-based AOPs, depending on its concentration and composition. At a low concentration, NOM can act as a co-oxidant, enhancing the formation of reactive intermediates and improving the oxidation efficiency. However, at a high concentration, NOM can scavenge reactive intermediates such as Fe(V) and Fe(IV), leading to reduced oxidation efficiency [62]. Additionally, NOM can form complexes with ferrate, reducing its availability for decomposition and the generation of reactive species [94]. Inorganic inhibitors can directly react with reactive species like •OH, consuming them and reducing their availability for oxidation reactions [95].

The simultaneous application of Fe(VI) and ozone in on-site wastewater treatment achieved 80.0% and 60.0% aniline removal, respectively [25]. The Fe(VI)-perborate system exhibited lower SMX removal in WWTP influent (35.5–63.9%) compared to that in pure water (75.0%), attributable to radical scavenging by abundant organic matter and ions in actual wastewater that suppress oxidative capacity. In addition, the actual sewage contains relatively high levels of COD and NH_3-N, which compete with pollutants for active free radicals [95].

Ferrate decomposition forms a negatively charged, porous, and hydrophilic ferric (hydro) oxide prefiltration layer on membranes, which can help to repel hydrophilic dissolved organic carbon and reduce membrane fouling [21]. The oxidative action of ferrate could also degrade aromatic and phenolic constituents in NOM into smaller organic molecules, reducing their membrane fouling potential [39]. However, ferrate can be toxic to certain microorganisms, potentially disrupting the microbial communities essential for biological treatment processes. Ferrate processes offer promising advantages in wastewater treatment. However, more laboratory research and long-term continuous operation results need further exploration.

5. Conclusions and Prospects

The oxidation enhancement in UV-TiO_2-Fe(VI) systems is caused by an improvement in quantum efficiency, with Fe(VI) capturing the photocatalytic electrons. In Fe(VI)-UV-TiO_2 systems, Fe(V) and Fe(IV), which have higher reactivity resulting from Fe(VI) reduction by light-generated electrons, are responsible for the high removal of pollutants. The contribution of Fe(VI) to H_2O_2-based AOPs is similar to that in Fe(VI) photocatalysis. A low H_2O_2 dosage and simultaneous dosing pattern gave Fe(V)- and Fe(IV)-dominated oxidation, where Fe(VI) is activated by electron transfer, whereas the Fenton-like reaction is triggered by a high H_2O_2 dosage and sequencing dosing pattern. The key bridge between Fe(VI) and Fenton-like reactions, ozonation, and sulfate radical-based AOPs is the effect of Fe(III) and Fe(II). Homogeneous catalysis can be realized using Fe(III) and Fe(II), whereas heterogeneous catalysis can be achieved by the successful catalysis of ozone and persulfate by the separated FeOOH/Fe_2O_3 particles.

The role of Fe can be changed by adjusting the operating factors such as pH, oxidant dosage, and dosing pattern. Additives with reducing or complexing abilities may also affect the change of Fe(III) and Fe(II) or the oxidation ability of Fe(V) and Fe(IV). An acidic pH accelerates the production of Fe(V)/Fe(IV) from Fe(VI) and maintains a higher Fe(II) concentration in the solution to activate the oxidants. The oxidant dosage mainly influences the efficiency with which the Fe species are utilized in the ferrate-AOP. The dosage in these systems can be optimized, and even the dominant oxidation contributors can vary due to changes in the Fe species. The dosing strategy includes the dosing sequence of ferrate and mother oxidants, which primarily affects the use efficiency of Fe(III)/Fe(II) by ozone, H_2O_2, and PMS, as well as the contribution of radicals in oxidizing pollutants. Some

reducing agents, such as hydroxylamine, can accelerate the conversion of Fe(III) into Fe(II), which has a higher catalytic ability, and complexing agents such as PAA may promote the oxidation ability of Fe(V)/Fe(IV).

Directions for future work on ferrate-AOP techniques include the following:

(1) In a practical wastewater process, the stability of reactive Fe species under the condition of variable wastewater composition might limit their large-scale practical application. The relevant research on Fe(VI) regulation was mainly carried out in pure water systems or for specific contaminants, with fewer studies on the removal of organic pollutants in actual wastewater. Based on the selective and nonselective oxidation of Fe(VI) and AOPs, further study of the different oxidation pathways triggered by adjusting the Fe species is required to guide research on natural organic matter resistance reduction during wastewater treatment. It is necessary to strengthen the research on the treatment efficiency of organic pollutants in actual wastewater.

(2) The development of cost-effective ferrate production methods and stable ferrate formulations is essential for its large-scale application. Combining ferrate-AOP with other treatment methods can address specific limitations and improve overall treatment performance. In situ production of high-valent Fe is required to develop more promising wastewater treatment processes based on ferrate-AOP techniques. Recently, new methods for generating Fe(IV)-based single-atom catalysts and the electrochemical synthesis of high-valence Fe species provide new prospects for generating Fe(VI). More efforts are needed to develop efficient Fe recycling and utilization in ferrate-AOP. While scaling up ferrate AOPs for large-scale applications faces economic and technological challenges, the potential benefits in terms of treatment efficiency and broad applicability make it a promising area for future research and development.

(3) A detailed characterization of the Fe(VI) decomposition byproducts is required. Although the residue particles from Fe(VI) activate ozone and PMS, their surface morphology and Fe valence are unclear. Moreover, a quantitative analysis of Fe(V) and Fe(IV) is required.

Author Contributions: Conceptualization, Y.W. and X.L.; investigation, Y.W., X.L. and X.M.; validation, P.K.; data curation, S.Q., J.H. and T.G.C.; writing—original draft preparation, Y.W. and X.L.; supervision, P.S. and L.Z.; writing—review and editing, Y.Z. and Y.Y.; project administration, Y.Y. All authors have read and agreed to the published version of the manuscript.

Funding: This study was financially supported by the Natural Science Foundation of Tianjin, China (21YFSNSN00160 and 22YFYSHZ00310), and the S &T Program of Hebei, China (22374203D).

Data Availability Statement: The data presented in this study are available upon request from the corresponding author.

Conflicts of Interest: The authors declare that they have no known competing financial interests or personal relationships that could have appeared to influence the work reported in this paper.

References

1. Yang, X.; Rosario-Ortiz, F.L.; Lei, Y.; Pan, Y.; Lei, X.; Westerhoff, P. Multiple Roles of Dissolved Organic Matter in Advanced Oxidation Processes. *Environ. Sci. Technol.* **2022**, *56*, 11111–11131. [CrossRef] [PubMed]
2. Song, Z.-M.; Xu, Y.-L.; Liang, J.-K.; Peng, L.; Zhang, X.-Y.; Du, Y.; Lu, Y.; Li, X.-Z.; Wu, Q.-Y.; Guan, Y.-T. Surrogates for on-line monitoring of the attenuation of trace organic contaminants during advanced oxidation processes for water reuse. *Water Res.* **2021**, *190*, 116733. [CrossRef] [PubMed]
3. Xiao, S.; Cheng, M.; Zhong, H.; Liu, Z.; Liu, Y.; Yang, X.; Liang, Q. Iron-mediated activation of persulfate and peroxymonosulfate in both homogeneous and heterogeneous ways: A review. *Chem. Eng. J.* **2020**, *384*, 123265. [CrossRef]

4. Cruz-Cruz, A.; Rivas-Sanchez, A.; Gallareta-Olivares, G.; González-González, R.B.; Cárdenas-Alcaide, M.F.; Iqbal, H.M.N.; Parra-Saldívar, R. Carbon-based materials: Adsorptive removal of antibiotics from water. *Water Emerg. Contam. Nanoplast.* **2023**, *2*, 2. [CrossRef]
5. Jiang, T.; Wang, B.; Gao, B.; Cheng, N.; Feng, Q.; Chen, M.; Wang, S. Degradation of organic pollutants from water by biochar-assisted advanced oxidation processes: Mechanisms and applications. *J. Hazard. Mater.* **2023**, *442*, 130075. [CrossRef]
6. Tufail, A.; Price, W.E.; Mohseni, M.; Pramanik, B.K.; Hai, F.I. A critical review of advanced oxidation processes for emerging trace organic contaminant degradation: Mechanisms, factors, degradation products, and effluent toxicity. *J. Water Process Eng.* **2021**, *40*, 101778. [CrossRef]
7. He, H.; Wang, L.; Liu, Y.; Qiu, W.; Liu, Z.; Ma, J. Improvement of Fe(VI) oxidation by NaClO on degrading phenolic substances and reducing DBPs formation potential. *Sci. Total Environ.* **2023**, *864*, 161080. [CrossRef]
8. Li, J.; Song, Y.; Jiang, J.; Yang, T.; Cao, Y. Oxidative treatment of NOM by selective oxidants in drinking water treatment and its impact on DBP formation in postchlorination. *Sci. Total Environ.* **2023**, *858*, 159908. [CrossRef]
9. Shao, B.; Don, H.; Feng, L.; Qiao, J.; Guan, X. Influence of sulfite/Fe(VI) molar ratio on the active oxidants generation in Fe(VI)/sulfite process. *J. Hazard. Mater.* **2020**, *384*, 121303. [CrossRef]
10. He, S.; Chen, Y.; Li, X.; Zeng, L.; Zhu, M. Heterogeneous Photocatalytic Activation of Persulfate for the Removal of Organic Contaminants in Water: A Critical Review. *ACS EST Eng.* **2022**, *2*, 527–546. [CrossRef]
11. Talaiekhozani, A.; Talaei, M.R.; Rezania, S. An overview on production and application of ferrate (VI) for chemical oxidation, coagulation and disinfection of water and wastewater. *J. Environ. Chem. Eng.* **2017**, *5*, 1828–1842. [CrossRef]
12. Yang, Y.; Ma, X.; Zhang, S.; Luo, X.; Geng, H.; Liu, J.; Tong, X.; Zhang, Y.; Sun, P.; Zhao, L. Synergistic action of ferrate and biochar in the removal of trichloroethylene from water: Little biochar addition, large ferrate activity improvement. *J. Environ. Chem. Eng.* **2023**, *11*, 110165. [CrossRef]
13. Jiang, J.Q. Research progress in the use of ferrate(VI) for the environmental remediation. *J. Hazard. Mater.* **2007**, *146*, 617–623. [CrossRef] [PubMed]
14. Sharma, V.K. Ferrate(VI) and ferrate(V) oxidation of organic compounds: Kinetics and mechanism. *Coord. Chem. Rev.* **2013**, *257*, 495–510. [CrossRef]
15. Sharma, V.K.; Zboril, R.; Varma, R.S. Ferrates: Greener oxidants with multimodal action in water treatment technologies. *Acc. Chem. Res.* **2015**, *48*, 182–191. [CrossRef] [PubMed]
16. Zhu, Y.; Nie, J.; Yang, X.; Guan, X. Degradation of tetrabromobisphenol A by ferrate(VI)-$CaSO_3$ process: Kinetics, products, and impacts on following disinfection by-products formation. *J. Hazard. Mater.* **2021**, *412*, 125297. [CrossRef]
17. Marbaniang, C.V.; Sathiyan, K.; McDonald, T.J.; Lichtfouse, E.; Mukherjee, P.; Sharma, V.K. Metal ion-induced enhanced oxidation of organic contaminants by ferrate: A review. *Environ. Chem. Lett.* **2023**, *21*, 1729–1743. [CrossRef]
18. Sharma, V.K.; Feng, M.; Dionysiou, D.D.; Zhou, H.C.; Jinadatha, C.; Manoli, K.; Smith, M.F.; Luque, R.; Ma, X.; Huang, C.H. Reactive High-Valent Iron Intermediates in Enhancing Treatment of Water by Ferrate. *Environ. Sci. Technol.* **2022**, *56*, 30–47. [CrossRef]
19. Wang, Y.; Wang, N.; Li, M.; Bai, M.; Wang, H. Potassium ferrate enhances ozone treatment of pharmaceutical wastewaters: Oxidation and catalysis. *J. Water Process Eng.* **2022**, *49*, 103055. [CrossRef]
20. Shaida, M.A.; Verma, S.; Talukdar, S.; Kumar, N.; Mahtab, M.S.; Naushad, M.; Farooqi, I.H. Critical analysis of the role of various iron-based heterogeneous catalysts for advanced oxidation processes: A state of the art review. *J. Mol. Liq.* **2023**, *374*, 121259. [CrossRef]
21. Zhang, S.; Jiang, J.-Q. Synergistic Effect of Ferrate with Various Water Processing Techniques-A Review. *Water* **2022**, *14*, 2497. [CrossRef]
22. Sharma, V.K.; Graham, N.J.; Li, X.Z.; Yuan, B.L. Ferrate(VI) enhanced photocatalytic oxidation of pollutants in aqueous TiO_2 suspensions. *Environ. Sci. Pollut. Res. Int.* **2010**, *17*, 453–461. [CrossRef] [PubMed]
23. Mura, S.; Malfatti, L.; Greppi, G.; Innocenzi, P. Ferrates for water remediation. *Rev. Environ. Sci. Bio/Technol.* **2016**, *16*, 15–35. [CrossRef]
24. Yu, J.; Jiao, R.; Sun, H.; Xu, H.; He, Y.; Wang, D. Removal of microorganic pollutants in aquatic environment: The utilization of Fe(VI). *J. Environ. Manag.* **2022**, *316*, 115328. [CrossRef]
25. Dar, A.A.; Pan, B.; Qin, J.; Zhu, Q.; Lichtfouse, E.; Usman, M.; Wang, C. Sustainable ferrate oxidation: Reaction chemistry, mechanisms and removal of pollutants in wastewater. *Environ. Pollut.* **2021**, *290*, 117957. [CrossRef]
26. Yu, J.; Sumita; Zhang, K.; Zhu, Q.; Wu, C.; Huang, S.; Zhang, Y.; Yao, S.; Pang, W. A Review of Research Progress in the Preparation and Application of Ferrate(VI). *Water* **2023**, *15*, 699. [CrossRef]
27. Dong, F.; Fu, C.; Feng, M.; Wang, D.; Song, S.; Li, C.; Lichtfouse, E.; Li, J.; Lin, Q.; Sharma, V.K. Simultaneous generation of free radicals, Fe(IV) and Fe(V) by ferrate activation: A review. *Chem. Eng. J.* **2024**, *481*, 148669. [CrossRef]
28. He, T.; Zhou, B.; Chen, H.; Yuan, R. Degradation of organic chemicals in aqueous system through ferrate-based processes: A review. *J. Environ. Chem. Eng.* **2022**, *10*, 108706. [CrossRef]

29. Fan, W.-Y.; Zhang, X.; Guo, P.-C.; Sheng, G.-P. Highly efficient removal of phosphonates by ferrate-induced oxidation coupled with in situ coagulation. *J. Hazard. Mater.* **2023**, *451*, 131104. [CrossRef]
30. Chu, Y.; Xu, M.; Li, X.; Lu, J.; Yang, Z.; Lv, R.; Liu, J.; Lv, L.; Zhang, W. Oxidation of emerging contaminants by S(IV) activated ferrate: Identification of reactive species. *Water Res.* **2024**, *251*, 121100. [CrossRef]
31. Zhang, X.; Zhu, X.; Li, H.; Wang, C.; Zhang, T. Combination of peroxymonosulfate and Fe(VI) for enhanced degradation of sulfamethoxazole: The overlooked roles of high-valent iron species. *Chem. Eng. J.* **2023**, *453*, 139742. [CrossRef]
32. Zhao, Z.; Xiang, L.; Wang, Z.; Liu, Y.; Damascene Harindintwali, J.; Bian, Y.; Jiang, X.; Schaeffer, A.; Wang, F.; Dionysiou, D.D. New insights into the Ferrate-Sulfite system for the degradation of polycyclic aromatic Hydrocarbons: A dual role for sulfite. *Chem. Eng. J.* **2023**, *477*, 147157. [CrossRef]
33. Pan, B.; Feng, M.; Qin, J.; Dar, A.A.; Wang, C.; Ma, X.; Sharma, V.K. Iron(V)/Iron(IV) species in graphitic carbon nitride-ferrate(VI)-visible light system: Enhanced oxidation of micropollutants. *Chem. Eng. J.* **2022**, *428*, 132610. [CrossRef]
34. Wang, Z.; Yang, X.; Du, Q.; Liu, T.; Dai, X.; Du, Y.; Zhang, H.; Zhou, P.; Xiong, Z.; Lai, B. Ferrate(VI)/percarbonate for the oxidation of micropollutants: Interactive activation and release of low-concentration hydrogen peroxide for efficient electron utilization. *J. Hazard. Mater.* **2024**, *469*, 134029. [CrossRef]
35. Wang, P.; Ding, Y.; Zhu, L.; Zhang, Y.; Zhou, S.; Xie, L.; Li, A. Oxidative degradation/mineralization of dimethyl phthalate (DMP) from plastic industrial wastewater using ferrate(VI)/TiO_2 under ultraviolet irradiation. *Environ. Sci. Pollut. Res. Int.* **2022**, *29*, 15159–15171. [CrossRef] [PubMed]
36. Yang, F.; Yin, C.; Zhang, M.; Zhu, J.; Ai, X.; Shi, W.; Peng, G. Enhanced Fe(III)/Fe(II) Redox Cycle for Persulfate Activation by Reducing Sulfur Species. *Catalysts* **2022**, *12*, 1435. [CrossRef]
37. Feng, M.; Jinadatha, C.; McDonald, T.J.; Sharma, V.K. Accelerated Oxidation of Organic Contaminants by Ferrate(VI): The Overlooked Role of Reducing Additives. *Environ. Sci. Technol.* **2018**, *52*, 11319–11327. [CrossRef]
38. Sharma, V.K.; Chenay, B.V.N. Heterogeneous photocatalytic reduction of Fe(VI) in UV-irradiated titania suspensions: Effect of ammonia. *J. Appl. Electrochem.* **2005**, *35*, 775–781. [CrossRef]
39. Liu, Y.; Yuan, Y.; Wang, Y.; Ngo, H.H.; Wang, J. Research and application of active species based on high-valent iron for the degradation of pollutants: A critical review. *Sci. Total Environ.* **2024**, *924*, 171430. [CrossRef]
40. Wang, J.; Liu, Y.; Feng, L.; Wang, Y.; Jia, H. New insights on UV-activated transformation of polynuclear Fe-hydroxide and iron(III) (hydr)oxide for enhanced removal of natural organic matter by ferrate. *J. Water Process Eng.* **2022**, *49*, 103183. [CrossRef]
41. Yuan, B.L.; Li, X.Z.; Graham, N. Reaction pathways of dimethyl phthalate degradation in TiO_2-UV-O_2 and TiO_2-UV-Fe(VI) systems. *Chemosphere* **2008**, *72*, 197–204. [CrossRef] [PubMed]
42. He, H.; Zhao, J. The efficient degradation of diclofenac by ferrate and peroxymonosulfate: Performances, mechanisms, and toxicity assessment. *Environ. Sci. Pollut. Res.* **2023**, *30*, 11959–11977. [CrossRef] [PubMed]
43. Ma, Y.; Zhang, K.; Li, C.; Zhang, T.; Gao, N. Oxidation of Sulfonamides in Aqueous Solution by UV-TiO_2-Fe(VI). *Biomed Res. Int.* **2015**, *2015*, 973942. [CrossRef] [PubMed]
44. Yuan, B.; Li, Y.; Huang, X.; Liu, H.; Qu, J. Fe(VI)-assisted photocatalytic degradating of microcystin-LR using titanium dioxide. *J. Photochem. Photobiol. A Chem.* **2006**, *178*, 106–111. [CrossRef]
45. Yang, T.; Mai, J.; Cheng, H.; Zhu, M.; Wu, S.; Tang, L.; Liang, P.; Jia, J.; Ma, J. UVA-LED-Assisted Activation of the Ferrate(VI) Process for Enhanced Micropollutant Degradation: Important Role of Ferrate(IV) and Ferrate(V). *Environ. Sci. Technol.* **2022**, *56*, 1221–1232. [CrossRef]
46. Zhang, H.; Luo, M.; Zhou, P.; Liu, Y.; Du, Y.; He, C.; Yao, G.; Lai, B. Enhanced ferrate(VI)) oxidation of sulfamethoxazole in water by CaO_2: The role of Fe(IV) and Fe(V). *J. Hazard. Mater.* **2022**, *425*, 128045. [CrossRef]
47. Zhu, J.; Yu, F.; Meng, J.; Shao, B.; Dong, H.; Chu, W.; Cao, T.; Wei, G.; Wang, H.; Guan, X. Overlooked Role of Fe(IV) and Fe(V) in Organic Contaminant Oxidation by Fe(VI). *Environ. Sci. Technol.* **2020**, *54*, 9702–9710. [CrossRef] [PubMed]
48. Luo, M.; Zhou, H.; Zhou, P.; Lai, L.; Liu, W.; Ao, Z.; Yao, G.; Zhang, H.; Lai, B. Insights into the role of in-situ and ex-situ hydrogen peroxide for enhanced ferrate(VI) towards oxidation of organic contaminants. *Water Res.* **2021**, *203*, 117548. [CrossRef]
49. Widhiastuti, F.; Fan, L.; Paz-Ferreiro, J.; Chiang, K. Oxidative treatment of bisphenol A by Fe(VI) and Fe(VI)/H_2O_2 and identification of the degradation products. *Environ. Technol. Innov.* **2022**, *28*, 102643. [CrossRef]
50. Li, W.; Tang, R.; Xiong, S.; Li, L.; Zhou, Z.; Su, L.; Gong, D.; Deng, Y. High-valent metal-oxo species in catalytic oxidations for environmental remediation and energy conversion. *Coord. Chem. Rev.* **2024**, *510*, 215840. [CrossRef]
51. Sharma, V.K.; O'Connor, D.B.; Cabelli, D.E. Sequential one-electron reduction of Fe(V) to Fe(III) by cyanide in alkaline medium. *J. Phys. Chem. B* **2001**, *105*, 11529–11532. [CrossRef]
52. Pan, B.; Liao, M.; Zhao, Y.; Lv, Y.; Qin, J.; Sharma, V.K.; Wang, C. Visible light activation of ferrate(VI) by oxygen doped $ZnIn_2S_4$/black phosphorus nanolayered heterostructure: Accelerated oxidation of trimethoprim. *J. Hazard. Mater.* **2023**, *460*, 132413. [CrossRef] [PubMed]

53. Cao, J.-Y.; Du, Y.; Dai, X.; Liu, T.; Wang, Z.-J.; Li, J.; Zhang, H.; Zhou, P.; Lai, B. Ferrate(VI)-based synergistic oxidation processes (Fe(VI)-SOPs): Promoted reactive species production, micropollutant/microorganism elimination, and toxicity reduction. *Chem. Eng. J.* **2024**, *489*, 151180. [CrossRef]
54. Lin, Y.; Qiao, J.; Sun, Y.; Dong, H. The profound review of Fenton process: What's the next step? *J. Environ. Sci.* **2025**, *147*, 114–130. [CrossRef]
55. Zhang, X.; Feng, M.; Luo, C.; Nesnas, N.; Huang, C.-H.; Sharma, V.K. Effect of Metal Ions on Oxidation of Micropollutants by Ferrate(VI): Enhancing Role of Fe^{IV} Species. *Environ. Sci. Technol.* **2021**, *55*, 623–633. [CrossRef]
56. Wang, J.; Kim, J.; Ashley, D.C.; Sharma, V.K.; Huang, C.H. Peracetic Acid Enhances Micropollutant Degradation by Ferrate(VI) through Promotion of Electron Transfer Efficiency. *Environ. Sci. Technol.* **2022**, *56*, 11683–11693. [CrossRef]
57. Wang, Y.; Zhang, Z.; Wang, X.; Guo, H.; Zhu, T.; Ni, B.-J.; Liu, Y. Percarbonate-strengthened ferrate pretreatment for enhancing short-chain fatty acids production from sewage sludge. *Sci. Total Environ.* **2023**, *904*, 166771. [CrossRef]
58. Xue, J.; Zhu, Z.; Zong, Y.; Huang, C.; Wang, M. Oxidative Degradation of Dimethyl Phthalate (DMP) by the Fe(VI)/H_2O_2 Process. *Acs Omega* **2019**, *4*, 9467–9472. [CrossRef]
59. Li, Y.N.; Duan, Z.H.; Wang, Y.F.; Yuan, Z.J.; Wang, G.Y. Preliminary treatment of phenanthrene in coking wastewater by a combined potassium ferrate and Fenton process. *Int. J. Environ. Sci. Technol.* **2018**, *16*, 4483–4492. [CrossRef]
60. Martins, A.F.; Frank, C.d.S.; Wilde, M.L. Treatment of a trifluraline effluent by means of oxidation-coagulation with Fe(VI) and combined Fenton processes. *Clean-Soil Air Water* **2007**, *35*, 88–99. [CrossRef]
61. Han, Q.; Dong, W.; Wang, H.; Ma, H.; Gu, Y.; Tian, Y. Degradation of tetrabromobisphenol A by a ferrate(vi)-ozone combination process: Advantages, optimization, and mechanistic analysis. *Rsc Adv.* **2019**, *9*, 41783–41793. [CrossRef] [PubMed]
62. Cheng, Y.; Zheng, F.; Dong, H.; Pan, F.; Sun, L.; Aleksandr, N.; Yuan, X. Enhanced oxidation of micropollutants by ozone/ferrate(VI) process: Performance, mechanism, and toxicity assessment. *J. Water Process Eng.* **2023**, *55*, 104211. [CrossRef]
63. Zhang, Y.-S.; Chen, X.-J.; Huang, X.-T.; Bai, C.-W.; Zhang, Z.-Q.; Duan, P.-J.; Chen, F. Buffer-free ozone-ferrate(VI) systems for enhanced oxidation of electron-deficient contaminants: Synergistic enhancement effects, systematic toxicity assessment, and practical applications. *Water Res.* **2024**, *260*, 121907. [CrossRef]
64. Prucek, R.; Tucek, J.; Kolarik, J.; Filip, J.; Marusak, Z.; Sharma, V.K.; Zboril, R. Ferrate(VI)-Induced Arsenite and Arsenate Removal by In Situ Structural Incorporation into Magnetic Iron(III) Oxide Nanoparticles. *Environ. Sci. Technol.* **2013**, *47*, 3283–3292. [CrossRef] [PubMed]
65. Gong, H.; Chu, W.; Xu, K.; Xia, X.; Gong, H.; Tan, Y.; Pu, S. Efficient degradation, mineralization and toxicity reduction of sulfamethoxazole under photo-activation of peroxymonosulfate by ferrate (VI). *Chem. Eng. J.* **2020**, *389*, 124084. [CrossRef]
66. Wu, S.; Li, H.; Li, X.; He, H.; Yang, C. Performances and mechanisms of efficient degradation of atrazine using peroxymonosulfate and ferrate as oxidants. *Chem. Eng. J.* **2018**, *353*, 533–541. [CrossRef]
67. Feng, M.; Cizmas, L.; Wang, Z.; Sharma, V.K. Synergistic effect of aqueous removal of fluoroquinolones by a combined use of peroxymonosulfate and ferrate(VI). *Chemosphere* **2017**, *177*, 144–148. [CrossRef]
68. Sheikhi, S.; Dehghanzadeh, R.; Maryamabadi, A.; Aslani, H. Chlorpyrifos removal from aqueous solution through sequential use of coagulation and advanced oxidation processes: By-products, degradation pathways, and toxicity assessment. *Environ. Technol. Innov.* **2021**, *23*, 101564. [CrossRef]
69. Pi, R.; Yang, Z.; Chai, J.; Qi, Y.; Sun, X.; Zhou, Y. Peroxysulfur species-mediated enhanced oxidation of micropollutants by ferrate(VI): Peroxymonosulfate versus peroxydisulfate. *J. Hazard. Mater.* **2024**, *475*, 134871. [CrossRef]
70. Dinc, O.; Waclawek, S.; Solis, R.R.; Dionysiou, D.D. Synergistic oxidative removal of sulfamethoxazole using Ferrate(VI) and peroxymonosulfate. *Chem. Eng. J.* **2024**, *488*, 151085. [CrossRef]
71. López-Vinent, N.; Cruz-Alcalde, A.; Moussavi, G.; del Castillo Gonzalez, I.; Hernandez Lehmann, A.; Giménez, J.; Giannakis, S. Improving ferrate disinfection and decontamination performance at neutral pH by activating peroxymonosulfate under solar light. *Chem. Eng. J.* **2022**, *450*, 137904. [CrossRef]
72. Liu, J.; Zhang, Z.; Chen, Q.; Zhang, X. Synergistic effect of ferrate (VI)-ozone integrated pretreatment on the improvement of water quality and fouling alleviation of ceramic UF membrane in reclaimed water treatment. *J. Membr. Sci.* **2018**, *567*, 216–227. [CrossRef]
73. Liu, J.; He, K.; Zhang, J.; Li, C.; Zhang, Z. Coupling ferrate pretreatment and in-situ ozonation/ceramic membrane filtration for wastewater reclamation: Water quality and membrane fouling. *J. Membr. Sci.* **2019**, *590*, 117310. [CrossRef]
74. Li, C.; Lin, H.; Armutlulu, A.; Xie, R.; Zhang, Y.; Meng, X. Hydroxylamine-assisted catalytic degradation of ciprofloxacin in ferrate/persulfate system. *Chem. Eng. J.* **2019**, *360*, 612–620. [CrossRef]
75. Chen, N.; Lee, D.; Kang, H.; Cha, D.; Lee, J.; Lee, C. Catalytic persulfate activation for oxidation of organic pollutants: A critical review on mechanisms and controversies. *J. Environ. Chem. Eng.* **2022**, *10*, 107654. [CrossRef]
76. Dong, H.; Li, Y.; Wang, S.; Liu, W.; Zhou, G.; Xie, Y.; Guan, X. Both Fe(IV) and Radicals Are Active Oxidants in the Fe(II)/Peroxydisulfate Process. *Environ. Sci. Technol. Lett.* **2020**, *7*, 219–224. [CrossRef]

77. Wang, Z.; Qiu, W.; Pang, S.; Gao, Y.; Zhou, Y.; Cao, Y.; Jiang, J. Relative contribution of ferryl ion species (Fe(IV)) and sulfate radical formed in nanoscale zero valent iron activated peroxydisulfate and peroxymonosulfate processes. *Water Res.* **2020**, *172*, 115504. [CrossRef]
78. He, C.; Zhang, X.; Lv, P.; Sui, H.; Li, X.; He, L. Efficient remediation of o-dichlorobenzene-contaminated soil using peroxomonosulfate-ferrate-FeS hybrid oxidation system. *J. Taiwan Inst. Chem. Eng.* **2021**, *119*, 23–32. [CrossRef]
79. Ji, F.; Li, C.; Wei, X.; Yu, J. Efficient performance of porous Fe_2O_3 in heterogeneous activation of peroxymonosulfate for decolorization of Rhodamine B. *Chem. Eng. J.* **2013**, *231*, 434–440. [CrossRef]
80. Zhang, Y.; Li, Z.; Yan, D.; Chen, H.; Zhang, M.; Wang, J.; Yang, G. Application of Fe(II)/peroxymonosulfate for efficient alkali lignin wastewater treatment: Insight into the synergistic interactions between redox reactions and coagulation. *Sep. Purif. Technol.* **2024**, *328*, 125037. [CrossRef]
81. Zeng, H.; Cheng, Y.; Repo, E.; Yu, X.; Xing, X.; Zhang, T.; Zhao, X. Trace Iron as single-electron shuttle for interdependent activation of peroxydisulfate and HSO_3^-/O_2 enables accelerated generation of radicals. *Water Res.* **2022**, *223*, 118935. [CrossRef] [PubMed]
82. Ren, Y.; Chu, Y.; Li, N.; Lai, B.; Zhang, W.; Liu, C.; Li, J. A critical review of environmental remediation via iron-mediated sulfite advanced oxidation processes. *Chem. Eng. J.* **2023**, *455*, 140859. [CrossRef]
83. Rao, D.; Dong, H.; Niu, M.; Wang, X.; Qiao, J.; Sun, Y.; Guan, X. Mechanistic Insights into the Markedly Decreased Oxidation Capacity of the Fe(II)/$S_2O_8^{2-}$ Process with Increasing pH. *Environ. Sci. Technol.* **2022**, *56*, 13131–13141. [CrossRef]
84. Meng, S.; Zhou, P.; Sun, Y.; Zhang, P.; Zhou, C.; Xiong, Z.; Zhang, H.; Liang, J.; Lai, B. Reducing agents enhanced Fenton-like oxidation (Fe(III)/Peroxydisulfate): Substrate specific reactivity of reactive oxygen species. *Water Res.* **2022**, *218*, 118412. [CrossRef] [PubMed]
85. Widhiastuti, F.; Fan, L.; Paz-Ferreiro, J.; Chiang, K. Oxidative degradation of bisphenol A in municipal wastewater reverse osmosis concentrate (ROC) using ferrate(VI)/hydrogen peroxide. *Process Saf. Environ. Prot.* **2022**, *163*, 58–67. [CrossRef]
86. Li, C.; Li, X.Z.; Graham, N. A study of the preparation and reactivity of potassium ferrate. *Chemosphere* **2005**, *61*, 537–543. [CrossRef] [PubMed]
87. Wu, Z.; Liu, A.; Yang, B.; Hu, X.; Repo, E.; Xiao, K.; Zeng, H.; Zhao, X. Cost-Effective $Fe^{IV}O^{2+}$ Generation for Antibiotics Removal in Electrochlorination of Mariculture Wastewater. *ACS EST Water* **2023**, *3*, 2512–2521. [CrossRef]
88. Topaloglu, A.K.; Kahraman, B.F. Textile dye removal in wastewater by peroxymonosulfate (PMS) activation on a zero-valent iron nanoparticle-modified ultrafiltration catalytic membrane (nZVI@PES). *Environ. Sci. Pollut. Res.* **2023**, *30*, 94779–94789. [CrossRef]
89. Sheikhi, S.; Jebalbarezi, B.; Dehghanzadeh, R.; Maryamabadi, A.; Aslani, H. Sulfamethoxazole oxidation in secondary treated effluent using Fe(VI)/PMS and Fe(VI)/H_2O_2 processes: Experimental parameters, transformation products, reaction pathways and toxicity evaluation. *J. Environ. Chem. Eng.* **2022**, *10*, 107446. [CrossRef]
90. Wang, S.; Hu, Y.; Wang, J. Strategy of combining radiation with ferrate oxidation for enhancing the degradation and mineralization of carbamazepine. *Sci. Total Environ.* **2019**, *687*, 1028–1033. [CrossRef]
91. Dong, H.; Wei, G.; Yin, D.; Guan, X. Mechanistic insight into the generation of reactive oxygen species in sulfite activation with Fe(III) for contaminants degradation. *J. Hazard. Mater.* **2020**, *384*, 121497. [CrossRef] [PubMed]
92. Gao, Y.; Zhou, Y.; Pang, S.-Y.; Wang, Z.; Shen, Y.-M.; Jiang, J. Quantitative evaluation of relative contribution of high-valent iron species and sulfate radical in Fe(VI) enhanced oxidation processes via sulfur reducing agents activation. *Chem. Eng. J.* **2020**, *387*, 124077. [CrossRef]
93. Manoli, K.; Li, R.; Kim, J.; Feng, M.; Huang, C.-H.; Sharma, V.K. Ferrate(VI)-peracetic acid oxidation process: Rapid degradation of pharmaceuticals in water. *Chem. Eng. J.* **2022**, *429*, 132384. [CrossRef]
94. Gao, L.; Guo, Y.; Zhan, J.; Yu, G.; Wang, Y. Assessment of the validity of the quenching method for evaluating the role of reactive species in pollutant abatement during the persulfate-based process. *Water Res.* **2022**, *221*, 118730. [CrossRef] [PubMed]
95. Chen, Z.; Li, C.; Su, J.; He, Z.; Xu, J.; Bian, Y.; Kim, H.; Guan, X. Enhanced sulfamethoxazole removal in water and wastewater by ferrate(VI)/perborate system via borate buffering. *J. Hazard. Mater.* **2025**, *492*, 138261. [CrossRef]

Disclaimer/Publisher's Note: The statements, opinions and data contained in all publications are solely those of the individual author(s) and contributor(s) and not of MDPI and/or the editor(s). MDPI and/or the editor(s) disclaim responsibility for any injury to people or property resulting from any ideas, methods, instructions or products referred to in the content.